

## Squeezing the Optical Near-Field Zone by Plasmon Coupling of Metallic Nanoparticles

J. R. Krenn, A. Dereux, J. C. Weeber, E. Bourillot, Y. Lacroute, and J. P. Goudonnet

*Laboratoire de Physique, Optique Submicronique, Université de Bourgogne, F-21011 Dijon, France*

G. Schider, W. Gotschy, A. Leitner, and F. R. Aussenegg

*Institut für Experimental Physik, Karl-Franzens Universität, A-8010 Graz, Austria*

C. Girard

*CEMES-CNRS, 29 rue Jeanne Marvig, BP 4347, F-31055 Toulouse, France*

(Received 7 October 1998)

We report on the experimental observation of near-field optical effects close to Au nanoparticles using a photon scanning tunneling microscope (PSTM). Constant height operation of the PSTM allowed an unprecedented direct comparison with theoretical computations of the distribution of the optical near-field intensity. An unexpected squeezing of the optical near field due to plasmon coupling was observed above a chain of Au nanoparticles. [S0031-9007(99)08708-6]

PACS numbers: 78.66.-w, 07.79.Fc, 42.25.Fx

The study of electromagnetic eigenmodes of small metal particles is motivated by fundamental research and by possible applications of the optical properties of such particles. Most experimental works involve a large number of small metal particles embedded inside a dielectric material or deposited on a surface. The particles were studied as disordered or ordered arrays [1,2]. In both cases, their optical properties were affected by statistical and/or collective effects. The shape and size inhomogeneities of a large array of small metal particles lead to a statistical averaging of the optical properties. Collective effects due to the multiple scattering of light between the particles become significant when the distance between the particles is reduced to the order of magnitude of the incident wavelength.

A recent experiment [3] determined the homogeneous linewidth of the plasmon resonance of metallic nanoparticles. In order to circumvent the inherent broadening associated to the large number of particles, a scanning near-field optical microscope (SNOM) was operated as a subwavelength local antenna to excite *single* nanoparticles in the *near-field* zone. The detection of the transmitted intensity took place in the *far-field* zone. This approach was inspired by experiments [4,5] where a photon scanning tunneling microscope (PSTM) detected the optical field close to small metal particles arranged in periodic arrays. Former studies exploited the plasmon fields of a thin metal film [6], or of a small particle deposited on thin metal film [7], to obtain near-field images of nonresonant structures.

In a PSTM as in SNOM, a nanometer-sized tip is piezoelectrically driven to scan close to the sample surface [8]. The distinct features of the PSTM setup relative to the SNOM are [9] (1) the use of a sharply elongated optical fiber as a local probe and not as a local emitter; and (2) the deposition of the sample on a glass prism illuminated total internal reflection. The nanometer-sized tip scanned above the sample surface frustrates the total reflection.

A PSTM detects, at the exit of the optical fiber, a signal proportional to the optical near field with a better spatial resolution than the forward scattered far field detected in classical optics or in transmission SNOM. At the micrometer scale, recent PSTM experiments [10] detected the scattering of the surface plasmons of a thin Ag film by 1  $\mu\text{m}$  diameter protrusions with rough craters (0.5  $\mu\text{m}$  diameter) in their middle. With the craters' depth being about 50 nm, the scattering by such nonresonant mesoscopic defects is explained on the basis of the Rayleigh hypothesis [11]. However, it was predicted theoretically and verified experimentally that the distribution of the optical near field close to dielectric objects had a completely different structure according to the mesoscopic or the nanoscopic sizes of the objects and that the near-field contrast close to dielectric nanoparticles depended on the incident polarization [12,13].

Such nontrivial behavior in the simple case of dielectric objects raises an important question about the correct understanding of the PSTM images recorded close to metal nanoparticles which are *resonant* at optical wavelengths.

To clarify this question, this paper presents the first comparison of experimental and theoretical near-field images of an *individual* Au nanoparticle deposited on a transparent substrate. The evolution of the optical near-field pattern is then studied further when a large number of identical particles are arranged as a linear chain. In this elementary transition toward the collective regime, the commonly spread intuitive interpretation of near-field distributions appears misleading if it is not critically checked against the solution of Maxwell equations.

The samples were fabricated by standard electron beam lithography using a JEOL 6400 scanning electron microscope (SEM) equipped with a lithography system (Raith). A substrate is obtained by spin coating polymethylmethacrylate (PMMA) films (60 nm thick) on a indium-tin-oxide (ITO) doped glass plate. A sample

pattern is then transferred to the substrate by electron beam exposure and chemical developing, resulting in a PMMA mask on which a 40 nm thick Au layer is evaporated in a high vacuum at a rate of 1 nm per sec. Removing the PMMA mask chemically resulted in Au particles remaining on the ITO glass plate at the sites defined by the electron-beam exposure.

The particles geometry was checked by SEM and atomic force microscope (AFM) measurements. The particles shapes were found to be akin of half oblate spheroids (cut plane on the substrate). Their typical sizes were a  $100 \times 100 \text{ nm}^2$  section and a 40 nm height. A microspectrometer located in the far field measured the single particles plasmon peak at the wavelength of 640 nm.

The fiber tips are obtained by a reproducible heat-and-pull technique resulting in a 20 nm tip apex diameter and a  $8^\circ$  taper angle. We used an AFM (digital instruments) which, after modifications, can also be operated as a PSTM. First, the AFM mode locates the nanostructures. The AFM tip is then replaced by an optical fiber tip which is approached to the sample until an exponential increase of the detected light intensity indicates the evanescent field above the sample surface. The plasmon resonance of the Au particles is associated to a large lateral variation of the intensity in the near-field zone so that the image acquisition cannot be performed efficiently at a constant intensity. The tip is thus scanned at a constant height above the sample surface while monitoring the light intensity level. Successive images are recorded while bringing the tip closer and closer to the sample surface. The series of images terminates when the tip touches a particle.

Theoretical modeling was performed in the framework of the Green's dyadic technique [14]. This numerical method is reliable to solve the Maxwell equations for the parameters of near-field optics. The technique is based on the knowledge of the Green's dyadic associated to a reference system which is the flat ITO glass surface. The procedure considers any object deposited on the surface as a perturbation discretized in direct space. First, the electric field is determined self-consistently inside the perturbations, a renormalization associated to the depolarization effect taking care of the self-interaction of each discretization cell [14]. The Huygens-Fresnel principle uses the values of the field inside the perturbations to compute the electric field elsewhere. In the computations of this paper, the incoming field  $\vec{E}_0$  was defined as in the experiments to be TM polarized and incident through the substrate under the condition of total internal reflection with an angle of incidence equal to  $55^\circ$ . At the wavelength in a vacuum fixed experimentally to be 633 nm, the dielectric function of the substrate is 2.37 while the one of Au is found in Ref. [15].

In Fig. 1, we compare a theoretical computation with an experimental PSTM image. In the simulation, the discretization cells of the  $100 \times 100 \times 40 \text{ nm}^3$  single Au particle were chosen to be  $10 \times 10 \times 10 \text{ nm}^3$  cubes

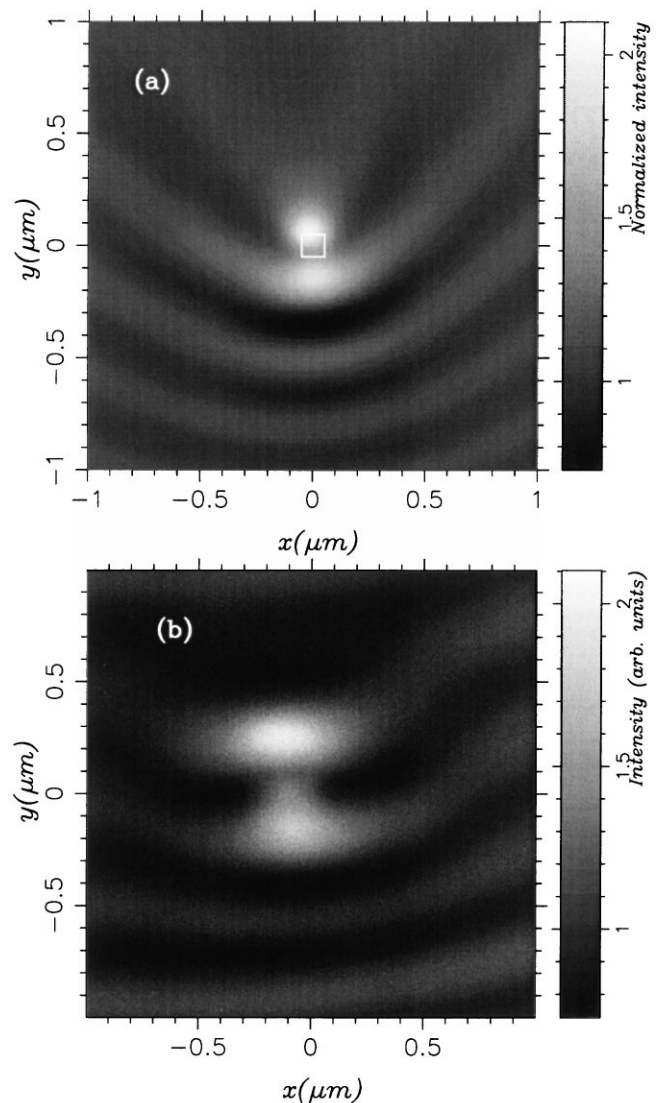


FIG. 1. Comparison of a theoretical computation (a) with an experimental PSTM image recorded at a constant height (b) of a Au particle ( $100 \times 100 \times 40 \text{ nm}^3$ ) deposited on a ITO substrate. The particle is centered at the origin of the coordinates system in the computation (a) (the surface projection of the model particle corresponds to the white square), while it is slightly translated to the left in the experimental image (b).

and the TM polarized incident field ( $\lambda = 633 \text{ nm}$ ) was adjusted to fit the experimental illumination conditions: the component of the incident wave vector which is parallel to the surface substrate is pointing mostly towards the  $y$  direction with a slight tilt to the upper left corner of the images. Previous works [12,13] have established the fact that the use of bare optical fibers results in a PSTM signal which is proportional to the intensity  $|\vec{E}|^2$  of the electric field associated to the optical wave that would exist in the absence of the tip. Taking the tip into account in the computation is not necessary unless one wants to assess precisely the smearing effect associated to the tip

as a function of the tip to the sample distance [16]. We therefore omitted the tip in the computation presented in Fig. 1(b) which maps the distribution of the normalized intensity of the electric field associated to the optical wave ( $|\vec{E}|^2/|\vec{E}_0|^2$ ) at the constant height  $z = 140$  nm above the glass substrate. This constant height does not correspond to the experimental tip to sample distance which was determined to be less than 45 nm since the experimental image displayed in Fig. 1 was the last one recorded before the tip touched the particle due to approaching the tip 5 nm closer to the sample. The height  $z = 140$  nm was found to provide the best agreement between the computed image and the experimental one after examining systematically the computed distribution patterns in planes parallel to the substrate surface at heights ranging between 0 and 200 nm. Since, in this height range, the distribution patterns are very similar from one plane to another, we defined the best agreement as the pattern exhibiting a contrast between the lowest and the highest intensity which is closest to the experimental image. We justify this procedure by the fact that we have not included the tip in the calculation. Since the tip integrates the optical field over a certain volume, the height  $z = 140$  nm should be interpreted as a rough modeling of the averaging process occurring inside the tip.

One remarks on an unprecedented good agreement between the patterns of the calculated and the experimental images. Since the simulation has not included the tip, the experimental image exhibits a broader and less contrasted pattern. The simulation successfully recovers the interference between the incident surface optical wave and the wave scattered by the Au particle. The computation fixes the exact position of the particle to be between the two central bright spots. The lower spot is a maximum of the backscattered surface wave while the upper one is related to forward scattering. First, we conclude that the near-field optical signature of a single Au resonant nanoparticle as detected by a PSTM is not the single spot found for nonresonant mesoscopic metal particles [10,11], and, second, is different from the signature of a dielectric structure with similar geometrical features [12,13]. A similar good agreement between the calculated and the experimental image has been found when the incident field is TE polarized (not shown for the sake of brevity).

We now examine in Fig. 2 the most elementary transition from the individual toward the collective regime by studying the optical near field close to a linear chain of 10 000 Au particles with identical shape and size as the particle studied in Fig. 1. We used the same illumination conditions as in Fig. 1 but, here, the component of the incident wave vector parallel to the surface substrate is aligned along the chain axis. If we neglect the effect due to some fabrication defect in the lower part of Fig. 2, we observe a periodic pattern of 85 nm diameter bright spots which appear *narrower* than the two 250 nm diameter brightest spots associated to the image of the single particle of Fig. 1. Relative to the incident wavelength of

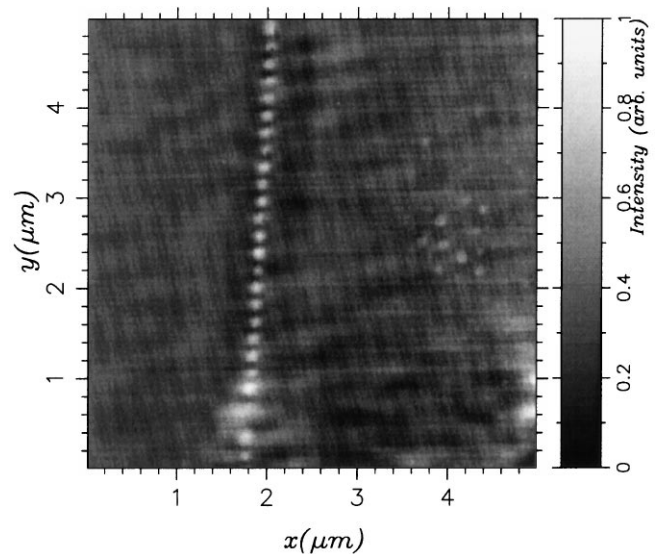


FIG. 2. Constant height PSTM image recorded above a chain of Au particles (individual size:  $100 \times 100 \times 40$  nm<sup>3</sup>) separated from each other by a distance of 100 nm and deposited on an ITO substrate.

633 nm used throughout the paper, this narrowing corresponds to an important squeezing of the optical near field along the chain. At this stage, it is tempting to attribute the positions of these spots to be on top of each Au particle. We tried to reproduce the phenomenon by numerical simulations.

To model the several thousand particles chains, we applied the numerical scheme to a row of 30 particles. In order to keep a reasonable calculation time, the  $100 \times 100 \times 40$  nm<sup>3</sup> Au pads were discretized by  $20 \times 20 \times 20$  nm<sup>3</sup> cubes (coarser than in Fig. 1). The computation maps the distribution of the normalized intensity ( $|\vec{E}|^2/|\vec{E}_0|^2$ ) at the constant height 140 nm above the glass substrate.

In Fig. 3(a), we show a zoom on the central part of Fig. 2 compared to the result of the calculation [Fig. 3(b)] above the central ten particles where the electric field is not too much influenced by the effects related to the finite size of the model. The theoretical modeling determines that the bright spots are not on top of the Au particles but localized between them, revealing the excitation of a hybrid electromagnetic eigenmode of the chain.

With Au particles, this mode is set up by plasmon coupling between individual particles (Fig. 4), giving rise to a lateral squeezing of the optical field. Indeed, the tip has integrated the detection of the optical field over its own volume at least. Consequently, the field distribution in the absence of the tip is probably narrower. The model calculation [Fig. 3(b)] confirms the fact that the spots are narrower than in the case of the single Au particle [Fig. 1(b)]. The calculated squeezing is not so narrow as in the experiment since the modeling involved only 30 particles instead of the 10 000 present in the

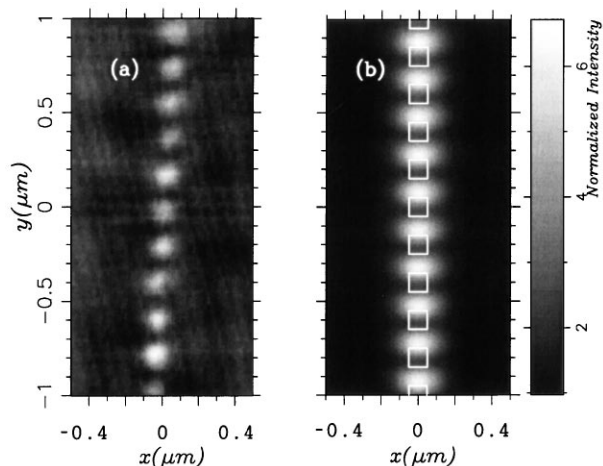


FIG. 3. (a) Zoom on the central part of Fig. 2. A comparison with a numerical simulation (b) shows that the bright spots are not on top of the Au particles (the surface projections of the particles correspond to the white squares). The intensity scale of experimental data (a) is normalized to the one of the numerical calculation (see text).

experiment. The squeezing probably increases as the chain length grows.

In conclusion, this paper provides an unprecedented comparison of a PSTM image with the theoretical distribution of the optical near-field intensity close to a single

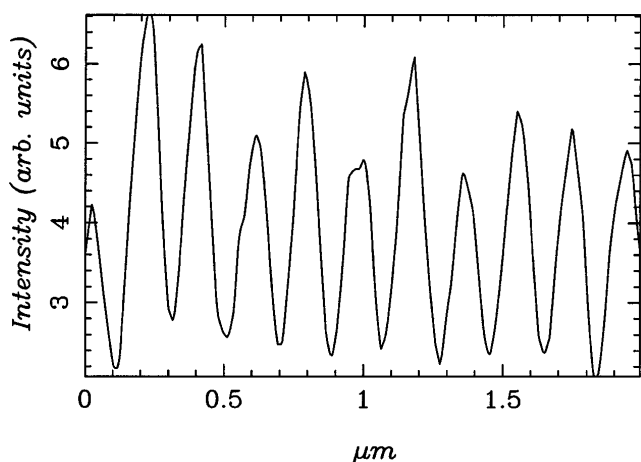


FIG. 4. Joining the point  $x = -0.043 \mu\text{m}$ ,  $y = -1.00 \mu\text{m}$  to the point  $x = 0.074 \mu\text{m}$ ,  $y = 1.00 \mu\text{m}$ ; this cut line across the data of Fig. 3(a) goes approximately over the maxima of each bright spot of Fig. 3(a).

metal particle. Added to preceding results [12,13], it shows that the PSTM is, up to now, the near-field optical device for which the images are proven to agree with Maxwell equations. A squeezed optical near field due to plasmon coupling was observed above a chain of Au nanoparticles. Modeling quantitatively this effect requires a calculation of the electromagnetic local density of states paying attention not only to the field along the axis of the chain but also to the width of the field perpendicular to this axis. This last aspect, depending on the size and shape of the particles, is not taken into account by theories involving ideal dipoles on a surface [17].

We acknowledge the support of the Region of Burgundy, of the French Ministry for Scientific Research, and of the Austrian Federal Ministry for Science, Technology Division.

- [1] C. Bohren and D. Huffman, in *Absorption and Scattering of Light by Small Particles* (J. Wiley, New York, 1983).
- [2] U. Kreibig and M. Vollmer, in *Optical Properties of Metal Clusters*, Springer Series in Material Science Vol. 25 (Springer-Verlag, Berlin, 1995).
- [3] T. Klar *et al.*, Phys. Rev. Lett. **80**, 4249 (1998).
- [4] J.R. Krenn *et al.*, Appl. Phys. A **61**, 541 (1995).
- [5] J.R. Krenn, R. Wolf, A. Leitner, and F.R. Aussenegg, Opt. Commun. **137**, 46 (1997).
- [6] M. Specht *et al.*, Phys. Rev. Lett. **68**, 476 (1992).
- [7] U.Ch. Fischer and D.W. Pohl, Phys. Rev. Lett. **62**, 458 (1989).
- [8] R.C. Reddick, R.J. Warmack, and T.L. Ferrell, Phys. Rev. B **39**, 767 (1989).
- [9] D. Courjon and C. Bainier, Rep. Prog. Phys. **57**, 989 (1994).
- [10] I.I. Smolyaninov, D.L. Mazzoni, and C.C. David, Phys. Rev. Lett. **77**, 3877 (1996).
- [11] A.V. Shchegrov, I.V. Novikov, and A.A. Maradudin, Phys. Rev. Lett. **78**, 4269 (1997).
- [12] C. Girard, A. Dereux, O.J.F. Martin, and M. Devel, Phys. Rev. B **52**, 2889 (1995).
- [13] J.C. Weeber *et al.*, Phys. Rev. Lett. **77**, 5332 (1996).
- [14] C. Girard and A. Dereux, Rep. Prog. Phys. **59**, 657 (1996).
- [15] E.D. Palik, *Handbook of Optical Constants of Solids* (Academic, San Diego, CA, 1985).
- [16] C. Girard, A. Dereux, O.J.F. Martin, and M. Devel, Phys. Rev. B **50**, 14 467 (1994).
- [17] M. Xiao, A. Zayats, and J. Siqueiros, Phys. Rev. B **55**, 1824 (1997).